solids

MDPI

Article

Intrinsic Defect-Related Photoluminescence in Single-Crystalline Tin Dioxide

Vadim F. Agekyan [1], Nikolai G. Filosofov [1], Alexey Yu. Serov [1] and Igor V. Shtrom [1,2,*]

[1] Faculty of Physics, St. Petersburg State University, St. Petersburg 199034, Russia
[2] Institute for Analytical Instrumentation of the Russian Academy of Sciences, St. Petersburg 198095, Russia
* Correspondence: i.shtorm@spbu.ru

Abstract

Photoluminescence studies of single-crystalline SnO_2 grown by chemical vapor transport from $SnCl_4$ and H_2O vapors were carried out in the visible spectral range. A non-trivial dependence of the 2.6 eV emission band on temperature and optical excitation level was observed. Based on the obtained data, the ionization energy of a shallow donor in SnO_2 was estimated to be 7 meV. Additionally, a model of energy levels and radiative transitions associated with shallow donors and intrinsic defects is proposed.

Keywords: tin dioxide crystals; photoluminescence; shallow donors; deep levels

1. Introduction

Crystalline tin dioxide (SnO_2) films, as well as tin-doped indium oxide (ITO), are among the most widely used transparent conducting oxides (TCOs) in modern semiconductor devices. Despite the appearance of alternative materials, such as $Zn_{1-x}Mg_xO$:Al layers, which demonstrate high conductivity [1], SnO_2-based films continue to dominate due to their excellent optical transparency, chemical stability, and high intrinsic defect concentrations that contribute to their metal-like conductivity, even in complex device architectures. The layered structures containing SnO_2, GeO_2, and TiO_2 are widely used as effective waveguides and Bragg reflectors in micro- and nanoscale optoelectronic systems. Both undoped and donor-doped SnO_2 films, with carrier concentrations up to 3×10^{20} cm^{-3}, are employed in photovoltaic modules [2]. Moreover, recent advancements in the SnO_2-based *p*-*n* junctions, including *p*-AlN:SnO_2 and *p*-AlN:SnO_2:In_2O_3 structures, highlight their potential for light-emitting diode (LED) and laser applications [3]. The bulk and nanocrystalline SnO_2 are widely used in gas sensing technologies [4]. Over the past decade, a significant number of studies have focused on the synthesis of SnO_2 nanocrystals and the characterization of their photoluminescence (PL) properties [5–14]. Two key factors influence the emission spectrum of nanocrystals: the quantum confinement effects and the critical role of surface states. These factors complicate interpretation of the emission mechanisms in nanocrystalline systems. While the exciton absorption and exciton PL of bulk SnO_2 crystals have been investigated in several studies [15,16], the light emission related to intrinsic defects in bulk material was not interpreted sufficiently. A commonly used synthesis method for SnO_2 nanocrystals is the direct oxidation of the tin metal, which leads to a large number of intrinsic defects. In such materials, the PL depends on intrinsic point defects. A series of free exciton lines near the fundamental band-to-band transition at 3.56 eV is observed in low-temperature absorption spectra of SnO_2 [15]. As for the emission spectra, even at cryogenic temperatures, the exciton luminescence is several orders of

check for updates

Academic Editor: Michael Reshchikov

Received: 28 October 2025
Revised: 28 November 2025
Accepted: 5 December 2025
Published: 11 December 2025

Citation: Agekyan, V.F.; Filosofov, N.G.; Serov, A.Y.; Shtrom, I.V. Intrinsic Defect-Related Photoluminescence in Single-Crystalline Tin Dioxide. *Solids* **2025**, *6*, 68. https://doi.org/10.3390/solids6040068

Copyright: © 2025 by the authors. Licensee MDPI, Basel, Switzerland. This article is an open access article distributed under the terms and conditions of the Creative Commons Attribution (CC BY) license (https://creativecommons.org/licenses/by/4.0/).

magnitude weaker than the broad visible-range bands. Such bands are typical for the oxygen-based crystals SnO_2, GeO_2, TiO_2, as well as for Cu_2O and Ag_2O. Higher oxides such as SnO_2 tend to exhibit oxygen deficiency, whereas the lower oxides like Cu_2O are characterized by an excess of oxygen. For example, in Cu_2O, broad PL bands are commonly attributed to copper vacancies and interstitial oxygen [17]. It was shown in [18] that an interstitial oxygen (O_i) and tin vacancies (V_{Sn}) are much less favorable energetically as compared to oxygen vacancy (V_O) and interstitial tin (Sn_i). Structural analysis suggests that the presence of one of these low-energy defects facilitates the formation of the other. Furthermore, theoretical studies [19] indicate that the donor levels associated with V_O and Sn_i lie below and above the conduction band minimum, respectively. As a result, the Sn_i donors are expected to remain ionized under most conditions.

Optical transitions from donor levels to high-lying empty bands could, in principle, contribute to light absorption, especially if they are dipole-allowed unlike the 3.56 eV band-to-band transition. However, no such absorption is observed, likely due to the fact that the next conduction band lies well above the lowest fundamental absorption edge [18]. This large energy separation, combined with low-energy intrinsic donor-type defects, explains how SnO_2 can simultaneously exhibit high electrical conductivity and transparency in the visible range. In this work, we present a PL study of the bulk SnO_2 single crystals. A more detailed study of the bulk crystal PL is essential to establish a baseline for understanding of nanocrystal PL behavior.

2. Experimental Details

The single crystals of SnO_2 used in this study were grown by chemical vapor transport from $SnCl_4$ and H_2O vapors. The vapors were carried into a reaction chamber by the argon gas flow. At a temperature of 1200 °C, twinned single crystals of tin dioxide several millimeters in size were formed due to the reaction $SnCl_4 + 2H_2O = SnO_2 + 4HCl$. The additional chlorine supply was used to suppress the secondary and spontaneous nucleation; thus, the growth of the large single crystals was stimulated. The crystals had well developed natural faces, which were not treated additionally during the experiment. The PL spectra of these crystals were measured over a temperature range of 5–230 K. The samples were mounted in a closed-cycle optical cryostat (Janis Research Co. Inc., Wilmington, MA, USA, SHI-4-1). The PL spectra were measured with a spectrometer (LOMO Photonics, St. Petersburg, Russia, MDR-204). Two types of excitation sources were used: a continuous-wave Plasma Lab., Ryazan, Russua, He-Cd laser HCL-49 (power 10 mW, photon energy 3.82 eV) for steady-state measurements; a Plasma Lab., Ryazan, Russua, pulsed nitrogen laser LCS-DTL-37 QT (pulse duration 6 ns, photon energy 3.68 eV, repetition rate 1 kHz, average power 10.5 mW, peak power 11 kW) for time-resolved measurements. The laser beam was focused to a spot 0.2 mm in diameter on the sample surface. The peak power density at the surface was estimated to be up to 10^7 W/cm^2.

3. Results and Discussion

We have established that annealing of SnO_2 single crystals at 750 °C and a pressure of 10^{-3} Torr for 3 h leads to strengthening and broadening of the bound exciton band in the absorption spectra (Figure 1a) as well as to the appearance of high conductivity at low temperatures. The reason for these changes may be an increase in O_v concentration during annealing, accompanied by formation of clusters differing from each other by the number of defects and their configuration. The inhomogeneous broadening of the bound exciton band is probably due to the dispersion of their binding energy with such clusters.

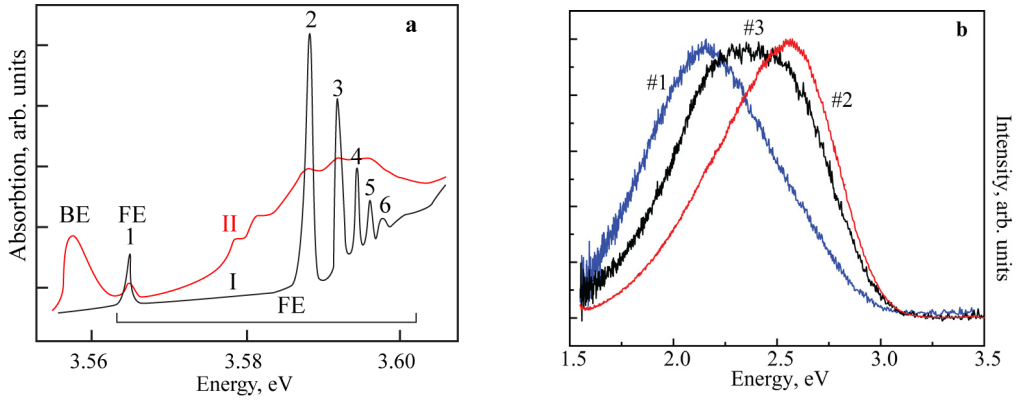

Figure 1. (**a**) Free (FE) and bound (BE) exciton absorption spectrum for the SnO_2 before (I) and after (II) high-temperature annealing, 1–6 are the principal quantum numbers of exciton lines; (**b**) normalized PL spectra of the SnO_2 samples #1, #2, and #3 under 3.82 eV continuous excitation. T = 5 K.

When considering the influence of annealing on optical spectra, two processes should be taken into account: an increase in defect concentration and a change in their properties. Oxygen vacancies can be neutral or singly and doubly positively charged. The relative concentrations of the vacancies with different charge states depend on the growth and after-growth treatment conditions. If annealing leads to a charge redistribution in favor of the vacancy that localizes excitons, an enhancement of the bound exciton band should be observed.

The energy of donor levels can be estimated from the exciton spectra. The binding energy of the lowest state of the free exciton (exciton Rydberg) in SnO_2 is 30 meV. Since the electron effective mass in SnO_2 is significantly smaller than the hole effective mass, the binding energy of the donor electron in the hydrogen-like approximation is estimated as 30 meV. The energy distance between the free and bound exciton levels in the SnO_2 spectra is 10 meV, which is in accordance with this estimate.

We now turn to the analysis of the PL of tin dioxide crystals in the visible spectral range. Figure 1b shows the spectra obtained under 3.82 eV continuous excitation at a power density of 1.5 W/cm^2. The relative intensities of the 2.0 and 2.6 eV bands vary significantly from sample to sample (samples #1, #2, and #3). As our samples were grown simultaneously in the same technological process, this difference is likely related to the vapor distributions inside the reaction chamber. Water molecules are much lighter than $SnCl_4$ molecules, and the partial pressure of water vapor is expected to be higher in a remote area of the reaction chamber. Thus, the defect concentrations depend on the position of the crystal growth point in the reaction chamber. This, in turn, results in different PL spectra from sample to sample. Figure 2a,b show the PL spectra of sample #1 at various temperatures and temperature dependence of the 2.0 and 2.6 eV band intensities. The intensity of the 2.0 eV band remains nearly constant at low temperature but decreases rapidly as the temperature increases. We suggest that the rapid thermal quenching of the 2.0 eV band occurs due to the ionization of shallow donor levels, from which this radiative transition takes place. As seen in Figure 2b, 2.0 eV band intensity decreases by half at 50 K. This means that the depth of the donor level can be estimated at about 7 meV. As mentioned above, the depth of the donor level related to the bound exciton (Figure 1a) is about 30 meV. This discrepancy suggests a different origin for the shallow level. According to [18], Sn_i has a very low formation energy and thus would exist in significant quantities. This suggests that the shallow donor level is formed by interstitial tin.

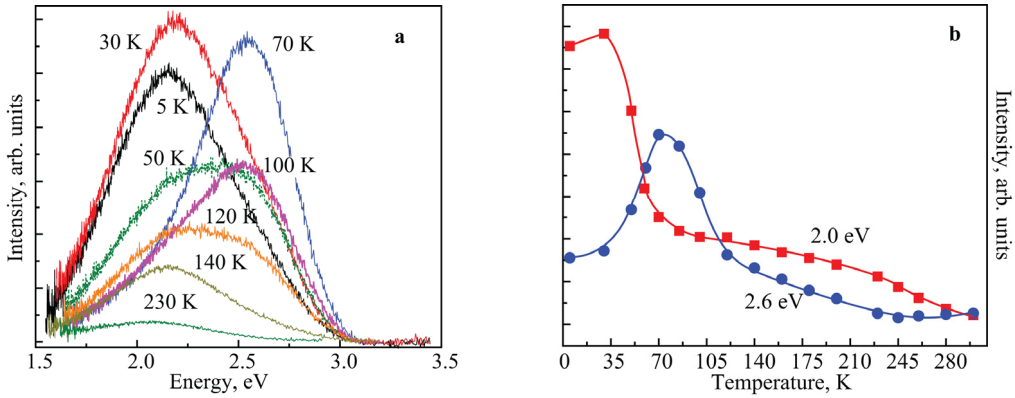

Figure 2. (**a**) PL spectra of sample # 1 at different temperatures under 3.82 eV continuous excitation. (**b**) Temperature dependences of the integral intensities of 2.0 and 2.6 eV bands in the PL spectra of sample # 1. Solid lines are guides for eye.

Figure 2 shows that the 2.6 eV band becomes more intense in the 5–30 K temperature range. This non-trivial temperature behavior of the 2.6 eV band intensity is governed by three factors: (i) the temperature dependence of the photoelectron capture cross section by donors, (ii) donor ionization, and (iii) non-radiative recombination. The electrons excited from the donor levels to the conduction band can participate directly in radiative recombination or be captured to deep levels. Simultaneous presence of both 2.0 and 2.6 eV bands in some low-temperature PL spectra (Figure 1b) supports the latter scenario (Figure 3). The 2.6 eV band that is getting stronger in the temperature range of 30–70 K appears due to the electron relaxation from the conduction band to a level, which is much deeper than the shallow donor level (Figure 3). At higher temperatures, the 2.6 eV band weakens due to thermally activated non-radiative recombination.

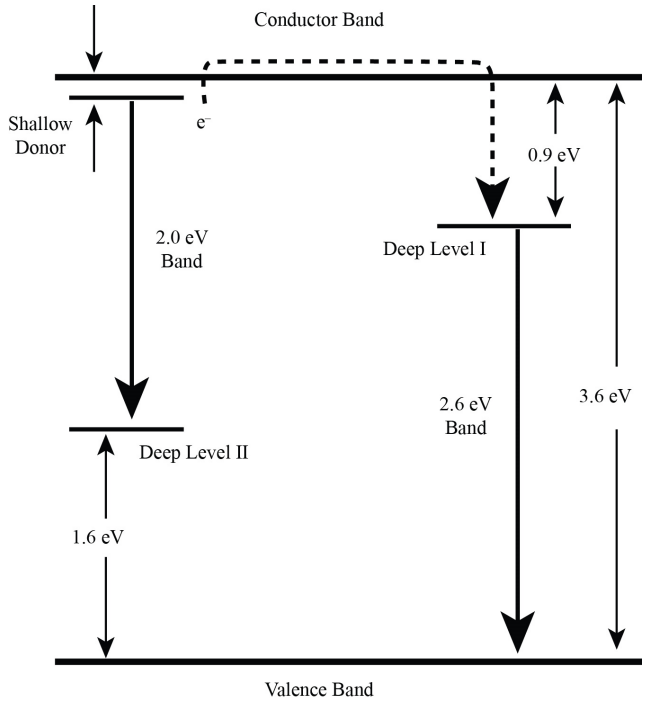

Figure 3. Scheme of energy levels and optical transitions in SnO_2. Dashed line indicates the electron transfer via the conduction band.

A question arises concerning the origin of defects responsible for the deep levels, as well as the defect where excitons, observed in the absorption spectra, are localized

(Figure 1a). Ab initio calculations performed in [18] show that the formation energies of the oxygen vacancy V_O and interstitial tin Sn_i are low, while the formation energies of tin vacancy V_{Sn} and interstitial oxygen O_i are much higher. The formation energies and charge states of these defects are such that V_{Sn} and O_i form the deep levels. The calculated formation energy of V_{Sn} was found to be greater than the formation energy of O_i. Based on these calculations, levels I and II (Figure 3) can be assigned to the tin vacancies and interstitial oxygen, respectively. A study of the exciton spectra revealed that annealing enhances the bound exciton band (Figure 1a). It is known that the annealing increases the oxygen deficiency in higher oxide crystals, leading to formation of oxygen vacancies. Thus, the bound exciton band can be formed by the excitons bound to oxygen vacancies.

PL measurements for sample #1 under pulsed N_2 laser excitation reveal strong dependence of the spectra on the excitation level (Figure 4a–c). The changes are insignificant up to the power density 10^6 W/cm^2 at T = 5 K (Figure 4a); however, with further increase in excitation, the 2.6 eV band intensity relatively increases. This indicates that at the excitation power density above 10^6 W/cm^2 the shallow donor states are saturated, and the photoelectrons relax effectively from the conduction band to the deep level I. Figure 4c shows the redistribution of intensity between the bands under the increasing excitation at T = 120 K. This can be explained by the transfer of the thermally activated electron from the deep level I to the non-radiative recombination center. As a result, only a weak 2.0 eV band at a relatively low excitation level is observed. With the increasing excitation, the non-radiative centers become saturated, and the 2.6 eV band strengthens. The dependence of the integral PL intensity of sample #1 versus the excitation power density is shown in Figure 5.

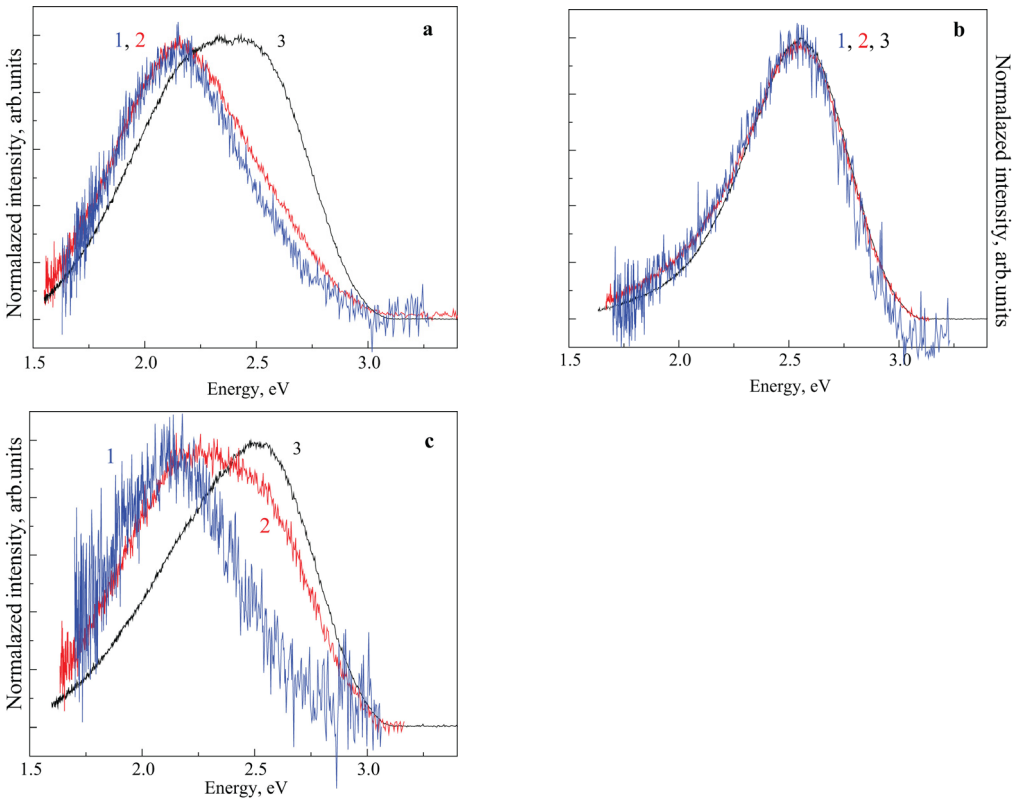

Figure 4. The PL spectra of sample #1 under 3.68 eV pulsed N_2 laser excitation at T = 5 (**a**), 70 (**b**) and 120 (**c**) K, and peak excitation power density 1.2 × 10^5 (1), 1.2 × 10^6 (2), and 0.9 × 10^7 (3) W/cm^2. The spectra are normalized to maximum intensity.

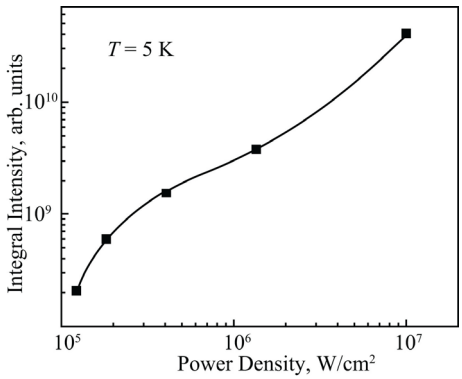

Figure 5. Integrated PL intensity versus the excitation power density for sample #1 under 3.68 eV pulsed N_2 laser excitation at T = 5 K. The solid line is a guide for the eye.

A flattening of the integral PL intensity vs. power density is observed between $4 \cdot 10^4$ and $2 \cdot 10^5$ W/cm^2 (Figure 5). We assume that this is due to the photo-induced activation of the non-radiative centers and their subsequent saturation.

Under continuous He–Cd laser excitation, the 2.0 eV band usually dominates in the low-temperature emission. This can be explained by the electron capture at the shallow donor level with subsequent optical transitions to the deep level located 0.9 eV above the valence-band maximum. The enhancement of the 2.6 eV band between 40 and 70 K results from the donor ionization, whereas its quenching at T > 70 K is likely due to thermally activated transfer of electrons from the deep radiative centers to the non-radiative ones.

4. Conclusions

In summary, the PL spectra of SnO_2 single crystals grown by the chemical vapor transport from $SnCl_4$ and H_2O vapors reveal two 2.0 eV and 2.6 eV bands related to shallow donor level and deep levels. We propose that shallow donor level is created by the interstitial tin atoms, while deep levels are related to tin vacancies and interstitial oxygen. The temperature decrease of the 2.0 eV band intensity along with the enhancement of the 2.6 eV band can be explained by the excitation of electrons from the shallow donor level into the conduction band, followed by their rapid capture at deep level. Transformation of the PL spectra under the increasing optical excitation depends strongly on the sample temperature. This reflects the interplay between donor ionization, electron capture by the deep centers, and non-radiative recombination processes.

Author Contributions: Conceptualization, V.F.A. and I.V.S.; formal analysis, A.Y.S. and I.V.S.; investigation, A.Y.S. and N.G.F.; methodology, A.Y.S., N.G.F. and V.F.A.; writing—original draft preparation, V.F.A. and I.V.S.; writing—review and editing, V.F.A., I.V.S., N.G.F. and A.Y.S.; supervision, I.V.S.; project administration, V.F.A. and I.V.S. All authors have read and agreed to the published version of the manuscript.

Funding: The authors acknowledge Saint Petersburg State University for a research project No. 129360164.

Data Availability Statement: The original contributions presented in this study are included in the article. Further inquiries can be directed to the corresponding author.

Conflicts of Interest: The author declares no conflicts of interest.

References

1. Fleischer, K.; Arca, E.; Smith, C.; Shvets, I.V. Aluminium doped $Zn_{1-x}Mg_xO$—A transparent conducting oxide with tunable optical and electrical properties. *Appl. Phys. Lett.* **2012**, *101*, 121918. [CrossRef]

2. Akagawa, M.; Fujiwara, H. Optical characterization of textured SnO_2:F layers using spectroscopic ellipsometry. *J. Appl. Phys.* **2012**, *112*, 083507. [CrossRef]
3. Liu, Y.S.; Hsieh, C.I.; Wu, Y.J.; Wei, Y.S.; Lee, P.M.; Liu, C.Y. Transparent p-type AlN:SnO_2 and p-AlN:SnO_2/n-SnO_2:In_2O_3 p-n junction fabrication. *Appl. Phys. Lett.* **2012**, *101*, 122107. [CrossRef]
4. Shen, W. Properties of SnO_2 based gas-sensing thin films prepared by ink-jet printing. *Sens. Actuators B Chem.* **2012**, *166–167*, 110. [CrossRef]
5. Choi, E.; Lee, D.; Shin, H.J.; Kim, N.; Valladares, L.D.L.S.; Seo, J. Role of oxygen vacancy sites on the temperature-dependent photoluminescence of SnO_2 nanowires. *J. Phys. Chem. C* **2021**, *125*, 14974. [CrossRef]
6. Costa, I.M.; Teodoro, M.D.; Zaghete, M.A.; Chiquito, A.J. Influence of the metastable state (V++) on the electronic properties of SnO_2 nanowires under the influence of light. *J. Appl. Phys.* **2020**, *128*, 115702. [CrossRef]
7. Zhou, J.X.; Zhang, M.S.; Hong, J.M.; Yin, Z. Raman spectroscopic and photoluminescence study of single-crystalline SnO_2 nanowires. *Solid State Commun.* **2006**, *138*, 242. [CrossRef]
8. Luo, S.; Chu, P.K. Origin of low-temperature photoluminescence from SnO_2 nanowires fabricated by thermal evaporation and annealed in different ambients. *Appl. Phys. Lett.* **2006**, *88*, 183112. [CrossRef]
9. Pramata, A.D.; Suematsu, K.; Quitain, A.T.; Sasaki, M.; Kida, T. Synthesis of Highly Luminescent SnO_2 Nanocrystals: Analysis of their Defect-Related Photoluminescence Using Polyoxometalates as Quenchers. *Adv. Funct. Mater.* **2017**, *27*, 1704620. [CrossRef]
10. Lee, E.J.; Ribeiro, C.; Giraldi, T.R.; Longo, E.; Leite, E.R.; Varela, J.A. Photoluminescence in quantum-confined SnO_2 nanocrystals: Evidence of free exciton decay. *Appl. Phys. Lett.* **2004**, *84*, 1745. [CrossRef]
11. Kazem, H.A.; Salman, H.I. The synthesis and characterization of SnO_2 nanostructure using hydrothermal method. *AIP Conf. Proc.* **2025**, *3395*, 050005.
12. Park, S.Y.; Zhu, K. Advances in SnO_2 for efficient and stable n–i–p perovskite solar cells. *Adv. Mater.* **2022**, *34*, 2110438. [CrossRef] [PubMed]
13. Jiao, J.; Zhang, Y.; Zhang, H.; Han, W.; Zhou, T.; Sun, Y.; Pang, S.; Wang, S.J. Enhanced ethanol sensing properties of SnO_2/$CdSnO_3$ heterostructure via a facile carbon incorporation strategy. *Alloys Compd.* **2025**, *1047*, 185061. [CrossRef]
14. Pham, V.T.; Le, T.H.; Chu, M.H.; Hoang, B.T.; Vu, T.T.; Tran, T.Q.H.; Nguyen, X.S.; Tran, N.K. Effects of annealing temperature on the structure, morphology, and photocatalytic properties of SnO_2/rGO nanocomposites. *Nanotechnology* **2021**, *32*, 015201. [CrossRef]
15. Aguekian, V.F.; Stepanov, Y.A.; Akai, I.; Karasawa, T.; Komatsu, T. Exciton luminescence in tin dioxide single crystals. *J. Phys. Soc. Jpn.* **1993**, *62*, 4516. [CrossRef]
16. Agekian, V.F.; Serov, A.Y.; Filosofov, N.G. Light emission from tin-dioxide crystals. *Semiconductors* **2014**, *48*, 442. [CrossRef]
17. Gastev, C.V.; Kuzmina, I.P.; Lazarevskaya, O.A.; Sokolov, N.S.; Yakovlev, N.L. Luminescence and optical detection of EPR-triplet states in CuO_2 crystals. *Sov. Phys. Solid State* **1983**, *25*, 2338.
18. Kiliç, Ç.; Zunger, A. On the possibility of p-type SnO_2. *Phys. Rev. Lett.* **2002**, *88*, 095501. [CrossRef] [PubMed]
19. Scanlon, D.O.; Watson, G.W. On the possibility of p-type SnO_2. *J. Mater. Chem.* **2012**, *22*, 25236. [CrossRef]

Disclaimer/Publisher's Note: The statements, opinions and data contained in all publications are solely those of the individual author(s) and contributor(s) and not of MDPI and/or the editor(s). MDPI and/or the editor(s) disclaim responsibility for any injury to people or property resulting from any ideas, methods, instructions or products referred to in the content.